

Image Gallery

List of images (For clarification of abbreviations, please refer to the abbreviation document)	Page
Image 1: Telangiectasia (C1)	4
Image 2: Reticular veins (C1)	4
Image 3: Varicose veins (C2)	4
Image 4: Oedema (C3)	4
Image 5: Pigmentation and dermatitis (C4a)	4
Image 6 Lipodermatosclerosis (C4b)	4
Image 7: Corona phlebectasia (C4c)	4
Image 8: Healed ulcer (C5)	4
Image 9: Active ulcer (C6)	4
Image 10: Adipose tissue in the saphenous compartment	5
Image 11: 'Egyptian eye' sign	5
Image 12: Colour image of the CFV	5
Image 13: Intergemellar vein	5
Image 14: Duplication of the GSV	5
Image 15: Hypoplasia of the GSV	5
Image 16: The terminal valve (TV) and preterminal valve (PTV)	6
Image 17: Alignment sign	6
Image 18: PAGSV	6
Image 19: Duplication of the SSV	6
Image 20: Termination of the SSV	6
Image 21: Common trunk formed by the SSV and MGV	6
Image 22: Superficial peroneal nerve vein	7
Image 23: Superficial peroneal nerve vein showing "string of beads" sonographic appearance	7
Image 24: Clinical image of the patient with varicosities in the posterolateral calf associated with an incompetent superficial peroneal nerve vein	7
Image 25: Incompetent GSV	7
Image 26: Competent GSV	7
Image 27: 'Mickey mouse' sign	7
Image 28: Spectral Doppler imaging of the CFV at the suprasaphenic and infrasaphenic levels	8
Image 29: Systolic reflux at the SFJ	8
Image 30: Systolic and diastolic reflux at the SFJ	8
Image 31: Anatomical variant of the SFJ with the GSV crossing posterior to the SFA	8
Image 32: Anatomical variant of the SFJ with the GSV passing through the gap between the SFA and PFA	8
Image 33: Variable termination of the GSV (SFJ: GSV-FV)	8
Image 34: Variable termination of the GSV (SFJ: GSV-DFV)	9
Image 35: Saphenous pulsation	9
Image 36: Continuous flow in the GSV	9
Image 37: Varicocoele	9
Image 38: Systolic reflux at the SPJ	9
Image 39: Systolic and diastolic reflux at the SPJ	9
Image 40: Paradoxical reflux in the vein of Giacomini	10
Image 41: Competent perforating vein	10
Image 42: Incompetent calf perforating vein	10

Image 43: Incompetent thigh perforating vein	10
Image 44: Re-entry perforating vein with systolic and diastolic inflow	10
Image 45: Incompetent perforating vein with systolic inflow and diastolic outflow	10
Image 46: Re-entry perforating vein with systolic outflow and diastolic inflow	11
Image 47: Incompetent perforating vein with systolic and diastolic outflow	11
Image 48: Vulval varicosities	11
Image 49: Clinical image of a patient with gluteal varicosities	11
Image 50: Gluteal perforating vein	11
Image 51: Clinical image of popliteal fossa vein	11
Image 52: Popliteal fossa perforating vein	12
Image 53: Clinical image of a patient with large varicosities on the posterolateral aspect of the thigh	12
Image 54: Posterolateral thigh perforating vein	12
Image 55: Clinical image of a patient with varicose veins on the lateral aspect of the calf attributed to incompetent SNV	12
Image 56: SNV	12
Image 57: Clinical image of a patient with an incompetent knee perforating vein, contributing to varicosities on the knee and the anterior aspect of the calf	12
Image 58: Incompetent knee perforating vein	13
Image 59: Clinical image of a patient with bilateral incompetent bone perforating veins	13
Image 60: Bone perforating vein	13
Image 61: Clinical image of a patient with incompetent LNVN in the left groin.	13
Image 62: Incompetent LNVN	13
Image 63: Ablated GSV following EVLA	13
Image 64: The GSV following cyanoacrylate glue ablation	14
Image 65: Strip-track haematoma post-GSV stripping surgery	14
Image 66: SFJ post high ligation	14
Image 67: SFJ with a GSV stump post ligation	14
Image 68: STP post avulsion	14
Image 69: Type I EHIT	14
Image 70: Type II EHIT	15
Image 71: Type III EHIT	15
Image 72: Type IV EHIT	15
Image 73: Mobile EHIT	15
Image 74: EGIT	15
Image 75: DVS	15
Image 76: STP	16
Image 77: Seroma	16
Image 78: Haematoma	16
Image 79: Sural nerve injury post EVLA	16
Image 80: Cutaneous necrosis	16
Image 81: Membranous fat necrosis	16
Image 82: Neovascularisation post ELVA	17
Image 83: Iatrogenic AVF	17
Image 84: Clinical image of the Type IV hypersensitivity in a patient who had cyanoacrylate glue ablation of the GSV	17
Image 85: Granuloma	17
Image 86: Cellulitis	17
Image 87: Clinical image of a patient with leg lymphoedema	17
Image 88 (a and b): Venous oedema	18

Image 89: Lymphodema	18
Image 90: Clinical image of a patient with leg lipoedema	18
Image 91: Lipoedema	18
Image 92: Lipoma	18
Image 93: AVM	19
Image 94: Venous malformation	19
Image 95: Muscle hernia	19
Image 96: Baker's cyst	19
Image 97: Neuroma	19
Image 98: Clinical image of a patient with Klippel Trenaunay syndrome (posterior and lateral views).	19
Image 99: Clinical image of a patient with Klippel Trenaunay syndrome (anterior view).	20
Image 100: Transmitted pulsatility in the CFV	20
Image 101: Transmitted pulsatility at the SFJ	20
Image 102: Room setup with a tiltable couch	21
Image 103: Room setup with a tiltable couch and an external monitor	21
Image 104: Room setup with a height adjustable couch, two step stool, low chair and an external monitor	21
Image 105: Room setup with a height adjustable couch, two step stool, yoga ball and an external monitor	21

Clinical signs of chronic venous disease

Image 1: Telangiectasia (C1)



Image 2: Reticular veins (C1)



Image 3: Varicose veins (C2)



Image 4: Oedema (C3)



Image 5: Pigmentation and dermatitis (C4a)



Image 6: Lipodermatosclerosis (C4b)



Image 7: Corona phlebectasia (C4c)



Image 8: Healed ulcer (C5)



Image 9: Active ulcer (C6)



Venous anatomy and duplex ultrasound scanning

Image 10: Adipose tissue in the saphenous compartment

Transverse view of the SSV at the upper calf (left) and mid-calf (right) level. There is only a small amount of adipose tissue contained within the saphenous compartment. However, the volume of adipose tissue increases towards the lower part of the calf due to gravity and orthostasis. This sonographic appearance is typically observed in women with lipoedema, progressively impairing the lymphatic drainage and leading to saphenous compartment syndrome.

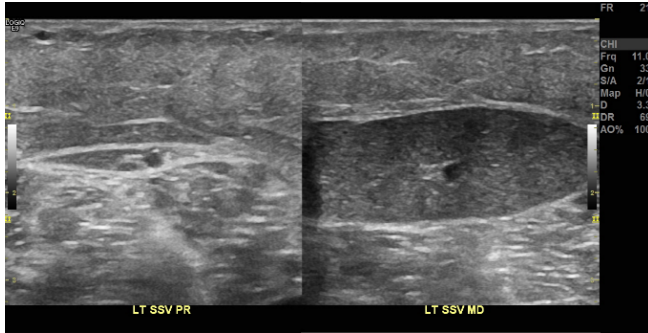


Image 11: Egyptian eye sign

Normal appearance of the GSV at the mid-thigh, showing that the saphenous vein is enclosed by the saphenous fascia and deep muscular fascia. It gives a characteristic sonographic appearance known as 'Egyptian eye' sign.



Image 12: Colour image of the CFV

A longitudinal view of the right CFV showing venous flow from the FV and DFV (labelled as PFV in the image) drain into the CFV. (blue: veins; red: artery)



Image 13: Intergemellar vein

Transverse image of the SSV at the upper calf level with an intergemellar vein coursing under the saphenous compartment between the heads of gastrocnemius muscles.



Image 14: Duplication of the GSV

B-mode image shows duplicated GSV at the mid-thigh level with doubled veins within the saphenous compartment.



Image 15: Hypoplasia of the GSV

B-mode image shows the hypoplasia of the GSV at the level of the distal thigh with a large epifascial tributary vein that functions as the GSV.



Image 16: The terminal valve (TV) and preterminal valve (PTV)

A longitudinal view of the left SFJ showing TV and PTV in the terminal section of the GSV just below its confluence with the CFV.



Image 17: Alignment sign

Transverse image of the upper thigh shows the ASV (labelled as AAGSV in the image) lies on the same axis as the superficial femoral artery (SFA) and FV. This "alignment sign" allows the ASV to be distinguished from the GSV.

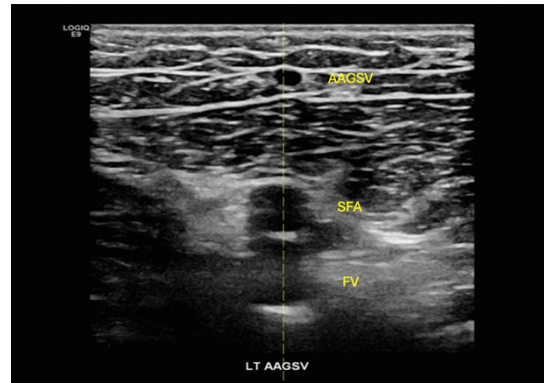


Image 18: PAGSV

B-mode ultrasound image of the PAGSV (labelled as PASV in the image) showing its anatomical relationship with the GSV, LNVN and ASV (labelled as AASV in the image).

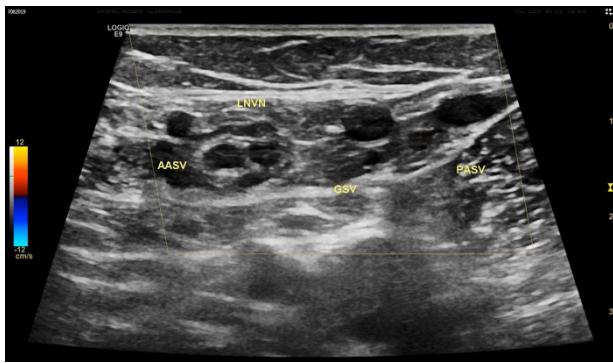


Image 19: Duplication of the SSV

B-mode image shows duplicated SSV at the level of mid-calf with both veins situated within the saphenous compartment.



Image 20: Termination of the SSV

B-mode image shows that the SSV and MGV join with the popliteal vein via separate junctions.

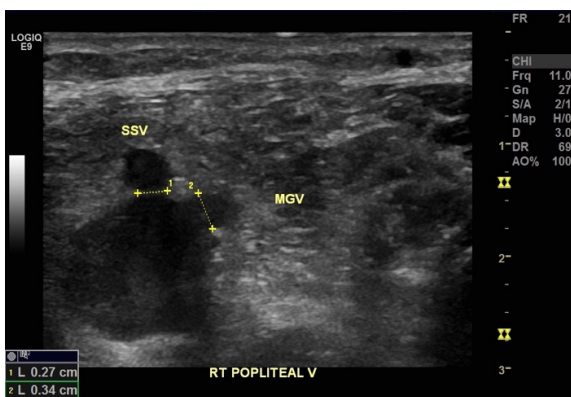


Image 21: Common trunk formed by the SSV and medial gastrocnemius veins (MGV).

Longitudinal B-mode image shows the SSV merges together with the MGV before joining the popliteal vein.

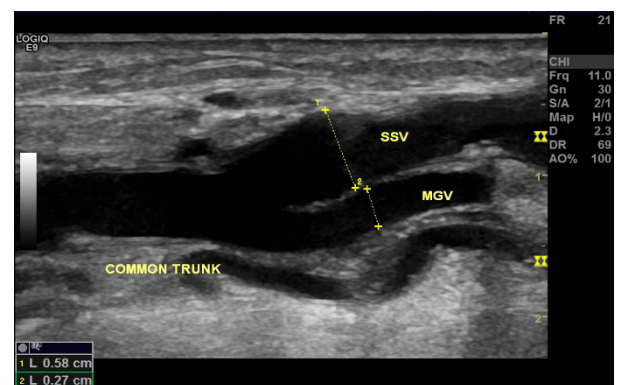


Image 22: Superficial peroneal nerve vein

Panoramic B-mode image of the superficial peroneal nerve vein (labeled as lat SSV in the image) which is situated in its own fascial compartment in the lateral calf.

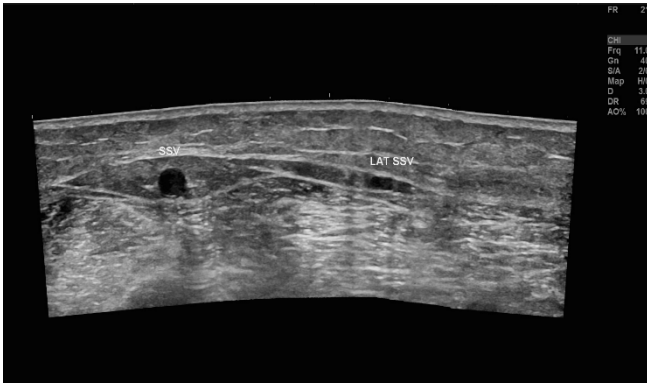


Image 23: Superficial peroneal nerve vein showing “string of beads” sonographic appearance

Colour Doppler image of the superficial peroneal nerve vein (labelled as lateral SSV in the image) displays a “string of beads” (-red-blue-red-) sonographic appearance.

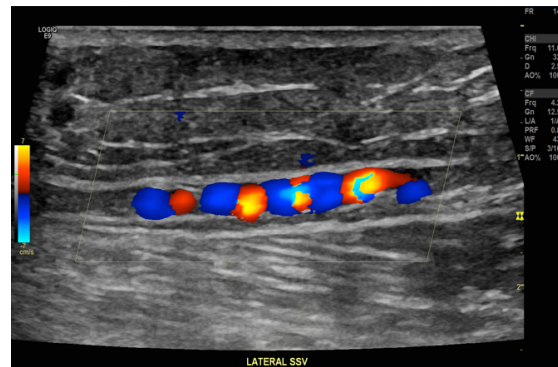


Image 24: Clinical image of the patient with varicosities in the posterolateral calf associated with an incompetent superficial peroneal nerve vein

Image 25: Incompetent GSV

Spectral Doppler imaging of the GSV with provocation manoeuvre. The sampled GSV segment demonstrates venous reflux upon the release of augmentation manoeuvre or diastolic phase following muscular contraction.

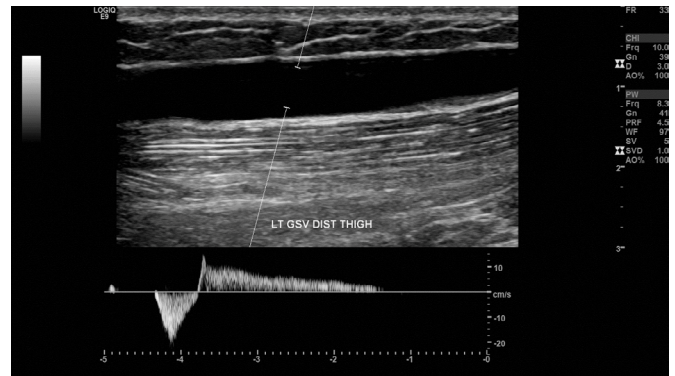


Image 26: Competent GSV

Spectral Doppler imaging of the GSV with provocation manoeuvre. The GSV demonstrates antegrade flow during distal augmentation manoeuvre and a brisk of physiological reversed flow on relaxation, indicating valvular competence in the sampled GSV segment.



Image 27: Mickey mouse sign

B-mode image of the left SFJ, mimicking a ‘Mickey mouse’ (Face:CFV; Right ear: GSV; Left ear: SFA).

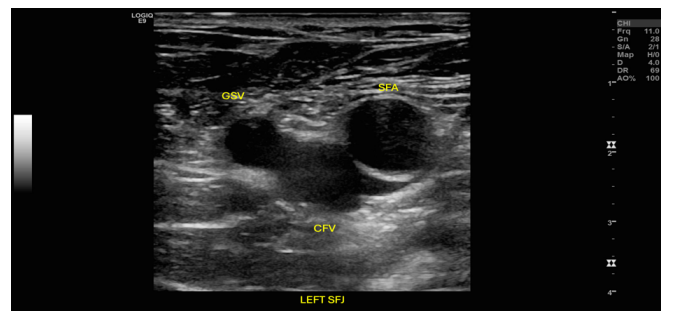


Image 28: Spectral Doppler imaging of the CFV at the suprasaphenic and infrasaphenic levels.

Left image: With the sample gate placed above the level of the SFJ, the CFV demonstrates reflux flow on the release of augmentation manoeuvre. Right image: With the sample gate placed in the CFV segment below the SFJ, it appears competent with no apparent reflux flow detected, suggesting CFV incompetence is likely related to the SFJ incompetence, and siphon effect of the GSV.

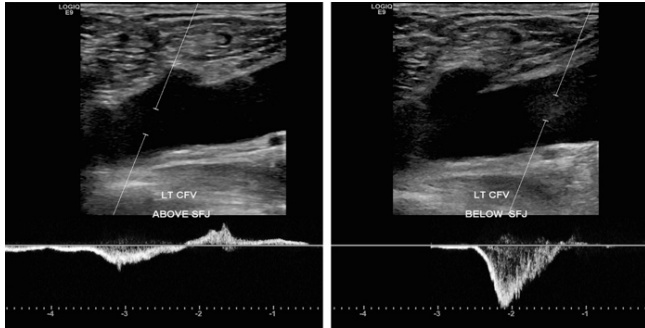


Image 29: Systolic reflux at the SFJ

In the presence of obstructive disease in the ipsilateral iliofemoral veins, reversed flow (systolic reflux) is demonstrated at the right SFJ during provocation manoeuvre, that is further drained via collateral veins. Brisk antegrade flow upon relaxation suggests competent terminal valves.

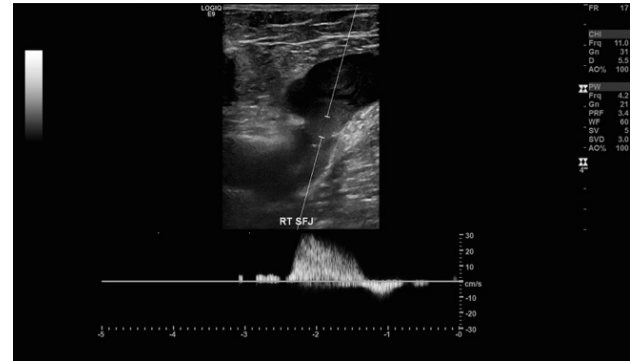


Image 30: Systolic and diastolic reflux at the SFJ

Spectral and colour Doppler imaging of the left SFJ. When provocation manoeuvre is applied, augmented flow travels from the CFV back to the GSV via the SFJ, known as systolic reflux. The diastolic flow is also in a reversed direction of prolonged duration, suggesting valvular incompetence at the SFJ. The coexistence of systolic and diastolic reflux occurs secondary to venous obstruction in the ipsilateral iliofemoral veins.

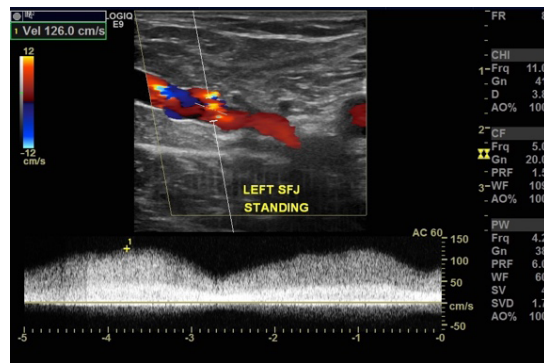


Image 31: Anatomical variant of the SFJ with the GSV crossing posterior to the SFA

B-mode image of the right SFJ. The classic 'mickey mouse' sign is not apparent; instead, the GSV joins the CFV on the lateral aspect after passing the SFA.

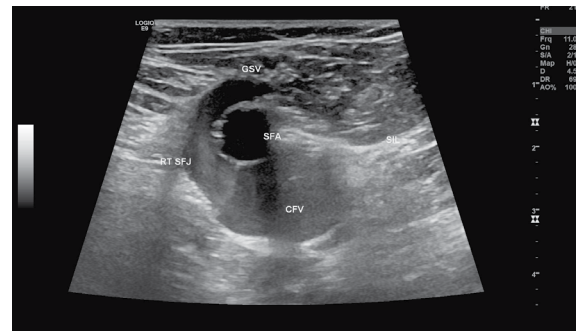


Image 32: Anatomical variant of the SFJ with the GSV passing through the gap between the SFA and PFA

Colour Doppler image of the left SFJ shows the terminal section of the GSV is sandwiched by the SFA and PFA (Profunda Femoris Artery).



Image 33: Variable termination of the GSV (SFJ: GSV-FV)

Longitudinal B-mode image of the right SFJ shows the GSV terminates into the FV instead of the CFV. (JX: termination of the FV into the CFV)



Image 34: Variable termination of the GSV (SFJ: GSV-DFV)

Transverse B-mode image of the right SFJ shows the GSV terminates into the DFV instead of the CFV.

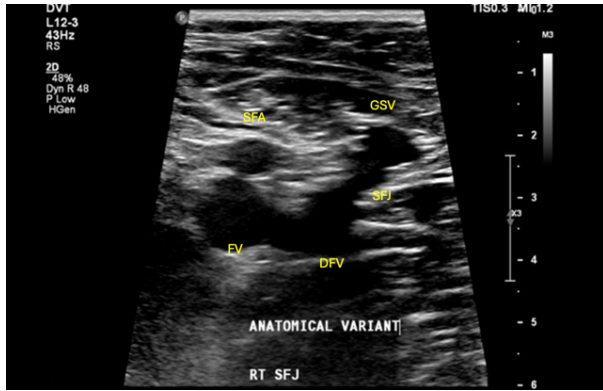


Image 35: Saphenous pulsation

At rest, the left GSV calf segment exhibits antegrade flow with a pulsatile pattern, indicative of saphenous pulsation. Notably, the spectral tracing shows no retrograde flow component, and the phenomenon is typically observed in patients with advanced stages of CVD/CVI, likely as a result of microcirculatory failure.

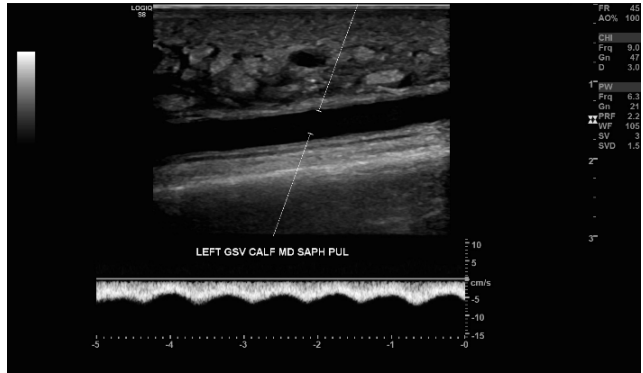


Image 36: Continuous flow in the GSV

At rest, the GSV demonstrates continuous antegrade flow due to venous obstruction in the femoropopliteal veins. Flow volume and velocity may increase when the patient lies in the supine position due to a reduction in the hydrostatic pressure gradient.

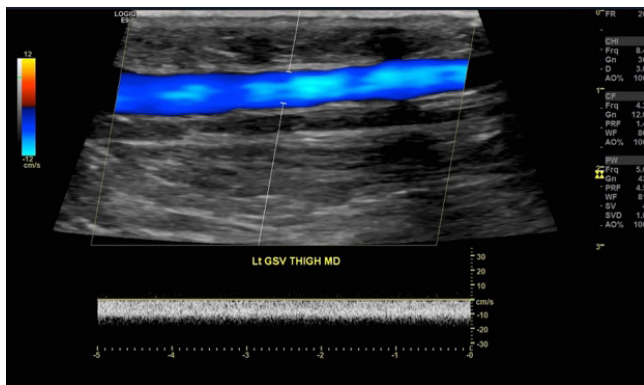


Image 37: Varicocele

Ultrasound image of varicocele shows dilated, tortuous veins within the scrotum, with increased echogenicity and noncompressibility, characteristic of a varicocele. The veins exhibit a "bag of worms" appearance, indicative of impaired venous drainage.

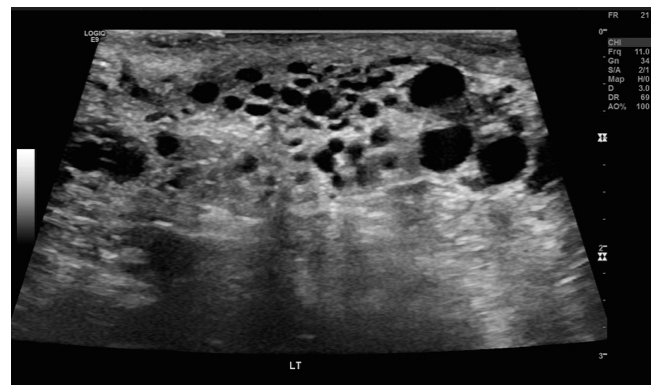


Image 38: Systolic reflux at the SPJ

During a provocation manoeuvre, augmented flow is observed traveling from the popliteal vein back to the SSV via the SPJ, indicating systolic reflux. However, upon relaxation, diastolic flow is absent on the spectral Doppler tracing, suggesting venous obstruction in the femoropopliteal vein and a competent SPJ.



Image 39: Systolic and diastolic reflux at the SPJ

During a provocation manoeuvre, augmented flow travels from the popliteal vein back into the SSV via the SPJ. Diastolic flow is also reversed and prolonged, indicating SPJ incompetence. The co-occurrence of systolic and diastolic reflux is due to venous obstruction in the femoropopliteal vein.

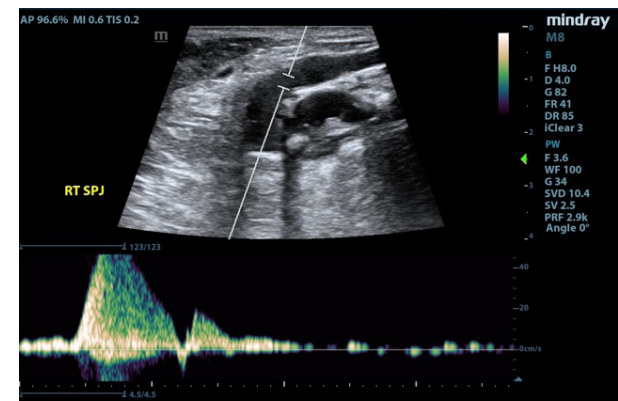


Image 40: Paradoxical reflux in the vein of Giacomini

The Giacomini's vein demonstrates flow in antegrade direction during both muscular systole and diastole. The diastolic flow most likely represents flow exiting out of the SPJ from the popliteal vein. This ascending reflux is known as paradoxical reflux.



Image 41: Competent perforating vein

An ultrasound image of a competent posterior tibial perforating vein shows inward flow during augmentation and brisk reversed flow upon relaxation (systolic: inward; diastolic: outward).

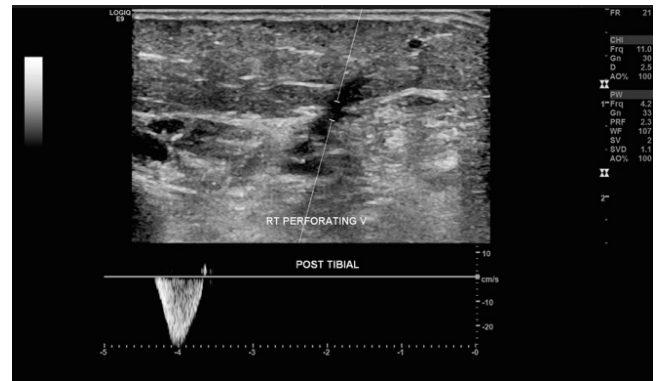


Image 42: Incompetent calf perforating vein

The posterior tibial perforating vein shows inward flow during augmentation and reversed flow of long duration upon relaxation, indicating perforating vein incompetence.

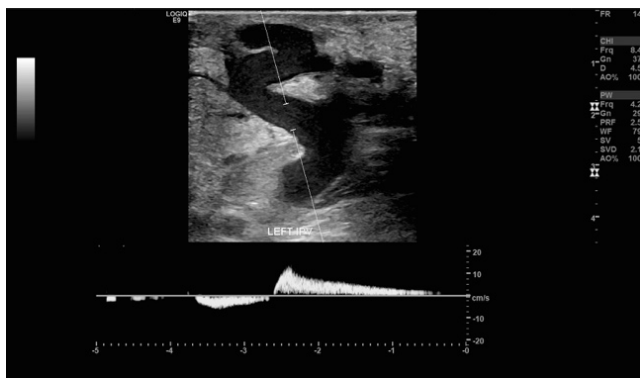


Image 43: Incompetent thigh perforating vein

This thigh perforating vein is identified as the source of reflux responsible for recurrent thigh varicosities. During a provocation maneuver, the flow direction is inward, but upon relaxation, prolonged reversed flow is observed on the spectral tracing, indicating perforating vein incompetence.

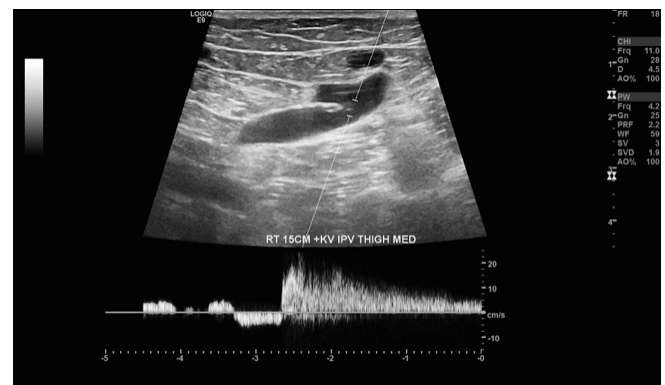


Image 44: Re-entry perforating vein with systolic and diastolic inflow

The lateral calf perforating vein demonstrates inward flow during and after augmentation (systolic: inward; diastolic: inward). This perforating vein functions as a re-entry point, draining superficial venous reflux.

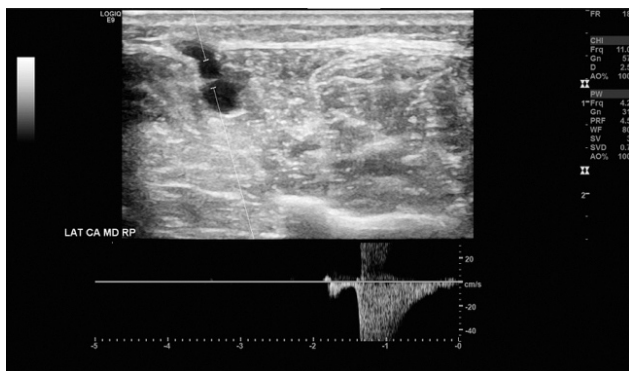


Image 45: Incompetent perforating vein or with systolic inflow and diastolic outflow

The mid-thigh perforating vein demonstrates inward flow during augmentation and outward flow upon relaxation (systolic: inward; diastolic: outward). This thigh perforating vein is identified as the source of reflux or an escape point.

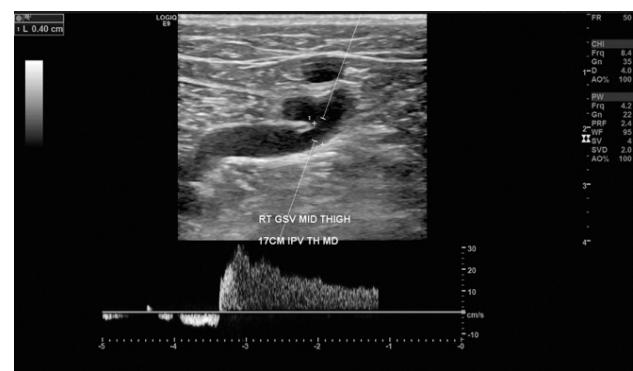


Image 46: Re-entry perforating vein with systolic outflow and diastolic inflow

The medial calf perforating vein shows outward flow during augmentation and inward flow upon relaxation (systolic: outward; diastolic: inward). This perforating vein functions as a re-entry point; however, systolic flow suggests the possibility of deep vein obstruction or incompetence.



Image 47: Incompetent perforating vein or with systolic and diastolic outflow

The paratibial perforating vein shows outward flow during and after augmentation manoeuvre (systolic: outward; diastolic: outward). This perforating vein is defined as the source of reflux or escape point. Additionally, its systolic flow suggests the possibility of deep vein obstruction or incompetence.

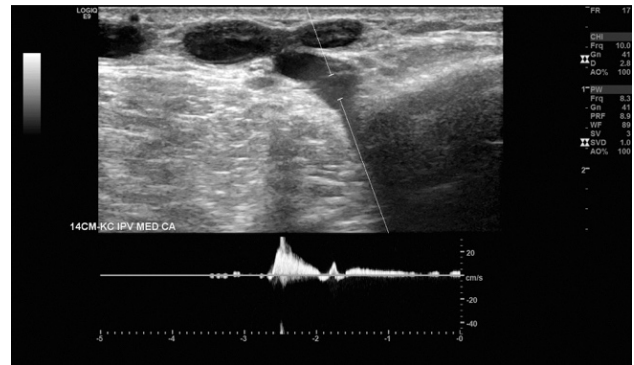


Image 48: Vulval varicosities

B-mode image of a patient with right sided vulval varicosities.

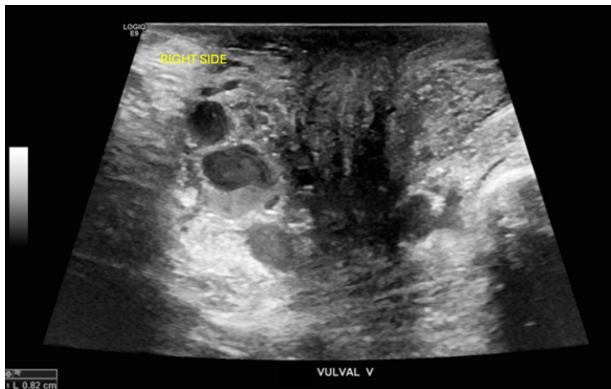


Image 49: Clinical image of a patient with gluteal varicosities

Image 50: Gluteal perforating vein

Spectral Doppler analysis of the gluteal perforating vein shows minimal inward flow during augmentation and reversed flow of prolonged duration on the release of augmentation manoeuvre, indicating perforating vein incompetence.

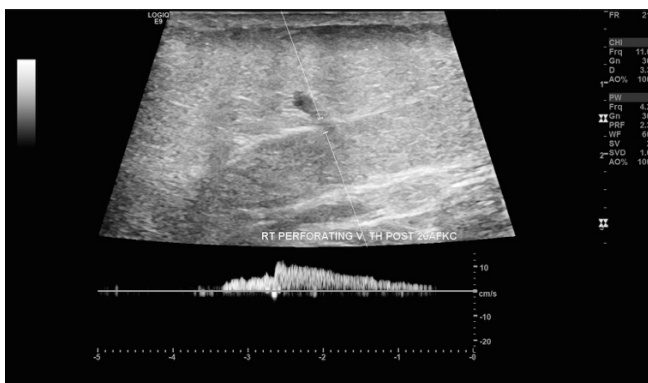


Image 51: Clinical image of popliteal fossa vein

Image 52: Popliteal fossa perforating vein

Spectral Doppler imaging of the popliteal fossa perforating vein shows inward flow during muscular contraction followed by high velocity, high volumed reflux flow upon relaxation.

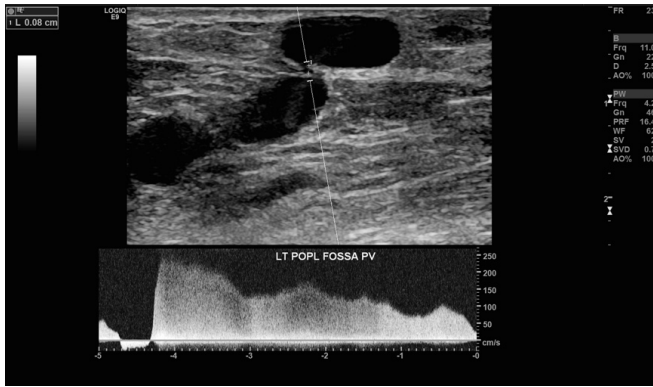


Image 53: Clinical image of a patient with large varicosities on the posterolateral aspect of the thigh

Image 54: Posterolateral thigh perforating vein

Spectral Doppler imaging of the left posterolateral thigh perforating vein shows inward flow (superficial to deep) during augmentation and outward flow (deep to superficial) of prolonged duration, indicating perforating vein incompetence.

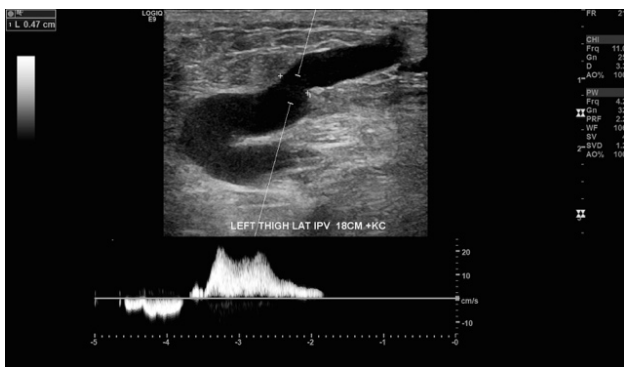


Image 55: Clinical image of a patient with varicose veins on the lateral aspect of the calf attributed to incompetent SNV.

Image 56: SNV

Spectral Doppler imaging of sciatic nerve varices shows antegrade flow during augmentation and reversed flow of prolonged duration on relaxation.

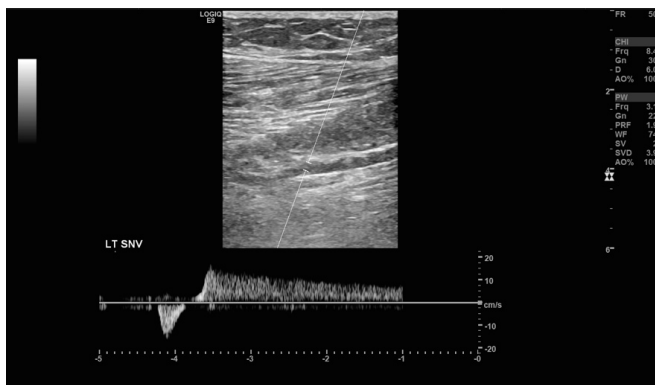


Image 57: Clinical image of a patient with an incompetent knee perforating vein, contributing to varicosities on the knee and the anterior aspect of the calf

Image 58: Incompetent knee perforating vein

Spectral Doppler imaging of the knee perforating vein shows reflux flow during muscular contraction and relaxation, indicating perforating vein incompetence.

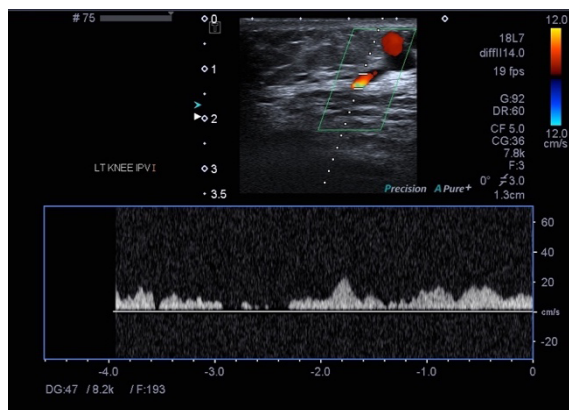


Image 59: Clinical image of a patient with bilateral incompetent bone perforating veins

Image 60: Bone perforating vein

B-mode image of a bone perforating vein shows a small osteolytic defect on the tibial shaft with diameter 0.6mm.

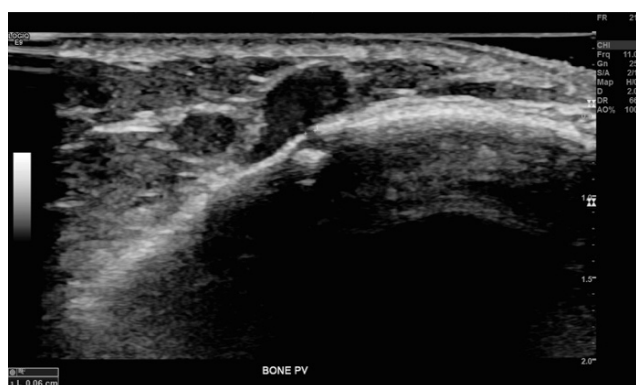


Image 61: Clinical image of a patient with incompetent LNVN in the left groin.

Venous incompetence in the LNVN result in varicosities along the medial upper thigh, with reflux flow extending further down into the GSV and its tributaries.

Image 62: Incompetent LNVN

Spectral Doppler imaging of the LNVN shows augmented flow in antegrade direction and reflux flow on relaxation.

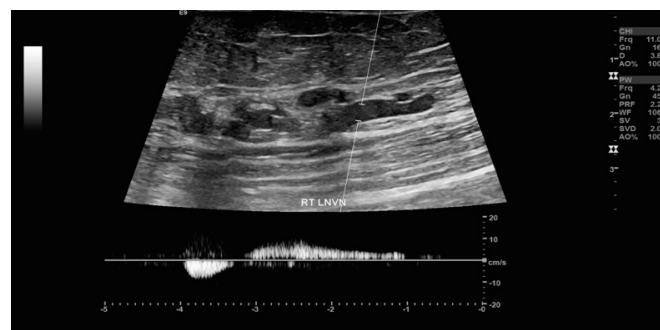


Image 63: Ablated GSV following EVLA

Spectral and colour Doppler imaging shows absence of flow signals in the GSV thigh segment that has undergone EVLA treatment.

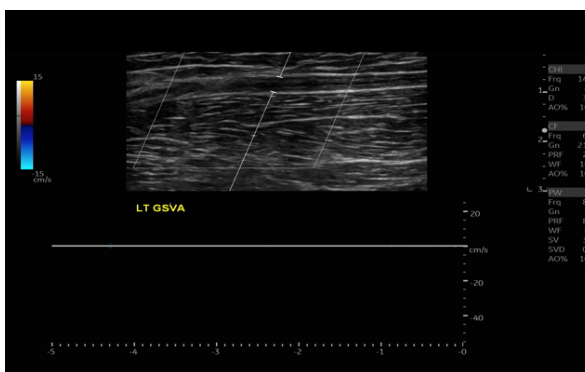


Image 64: The GSV following cyanoacrylate glue ablation
B-mode image of the GSV shows acoustic shadowing caused by the cyanoacrylate glue.



Image 65: Strip-track haematoma postGSV stripping surgery

Postoperative image of the saphenous compartment showing strip-track haematoma following GSV stripping surgery.

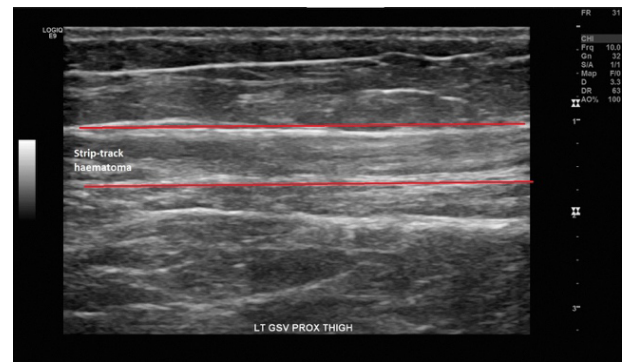


Image 66: SFJ post high ligation

Postoperative image of the former SFJ following flush ligation.

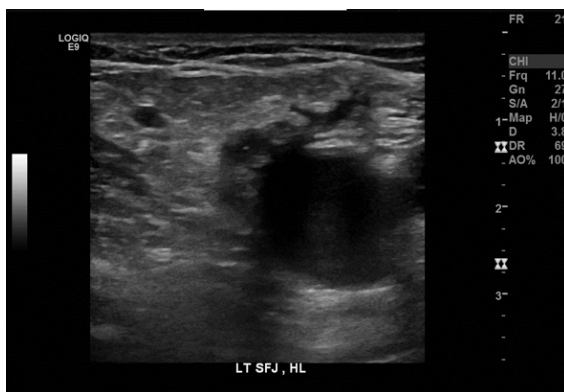


Image 67: SFJ with a GSV stump post ligation

Postoperative image of the left SFJ following low ligation with a residual GSV stump.

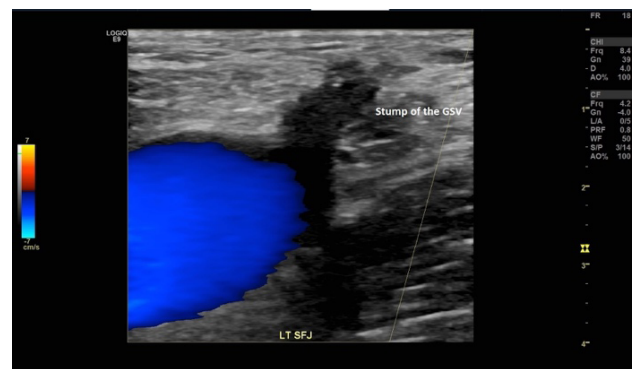


Image 68: STP postavulsion

Ultrasound image of an avulsed thigh tributary vein with superficial venous thrombosis and absence of vascularity.



Image 69: Type I EHIT

Type I EHIT where the thrombosis stops at the SFJ.

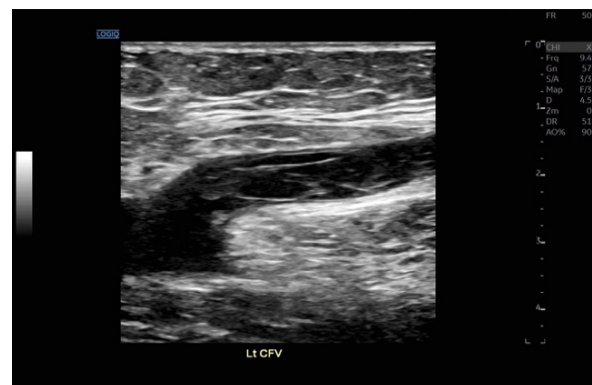


Image 70: Type II EHIT

Type II EHIT where the thrombus extends into the CFV causing less than 50% of luminal reduction.



Image 71: Type III EHIT

Type III EHIT where the thrombus extends into the CFV causing greater than 50% of luminal reduction.



Image 72: Type IV EHIT

Type IV EHIT where the thrombus extends into the CFV causing complete occlusion of the CFV.

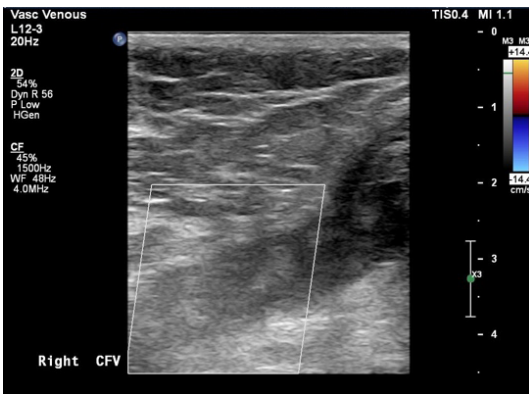


Image 73: Mobile EHIT

B-mode image displaying a mobile type of the EHIT reveals a flap at the SFJ following the EVLA procedure.

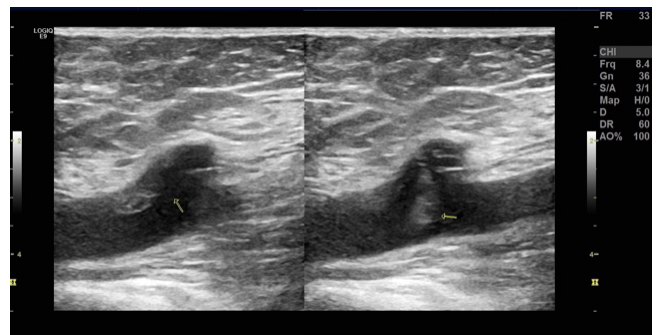


Image 74: EGIT

Extension of the glue into the left popliteal vein following cyanoacrylate glue ablation of the SSV.



Image 75: DVS

After the injection of foam to medial calf tributary veins, DVS is present in the posterior tibial perforating vein located at 8cm above the level of medial malleoli, extending into the posterior tibial veins. The veins with DVS appear to have similar appearance to those with DVT with internal echogenicity.

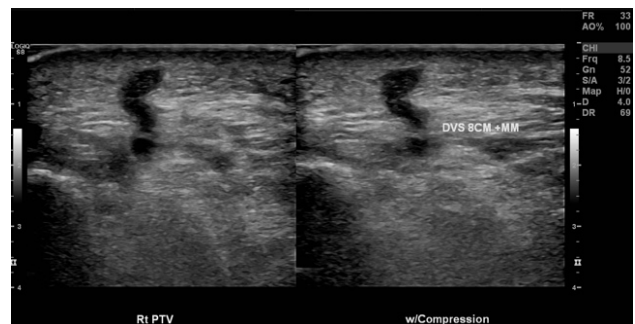


Image 76: STP

An acute superficial thrombus spontaneously formed in the large varicose tributary vein, showing mixed echogenicity.

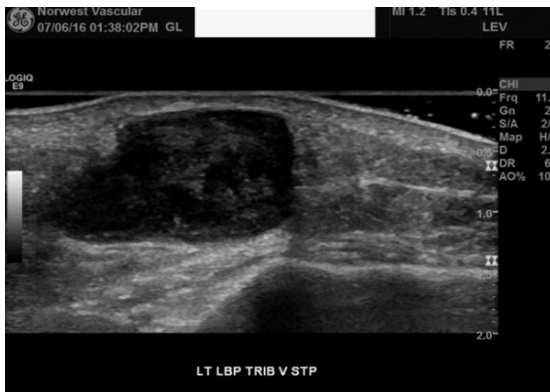


Image 77: Seroma

Ultrasound image of an inguinal seroma that is formed after the SFJ ligation and stripping of the GSV.

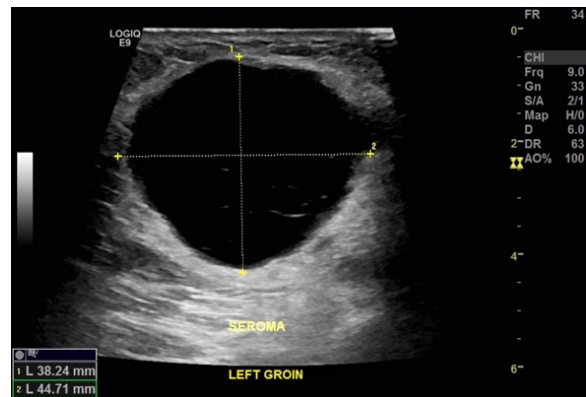


Image 78: Haematoma

Ultrasound image showing a large, well defined, oval-shaped haematoma formed after the SFJ ligation. It has mixed echogenic content, whorled appearance in the anterior region and a fluid component along the posterior wall.



Image 79: Sural nerve injury post EVLAT

Ultrasound image of an iatrogenic injury to the sural nerve resulting from the SSV ablation procedure, showing a thickened nerve and partial loss of the fascicular pattern.

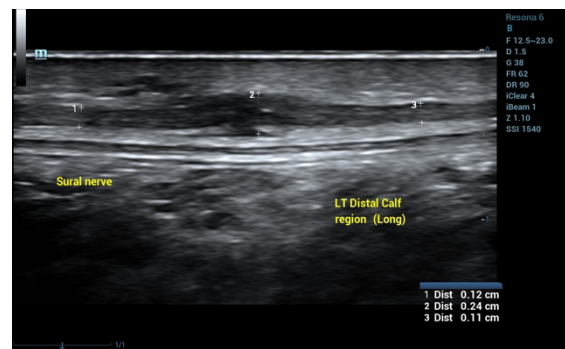


Image 80: Cutaneous necrosis

Cutaneous necrosis after injection with polidocanol 1% into telangiectasia. Superficial ulceration is present on the anterior aspect of the calf at week 2.



Image 81: Membranous fat necrosis

Ultrasound image of fat necrosis as a result of extravasation of sclerosant into the subcutaneous adipose tissue.

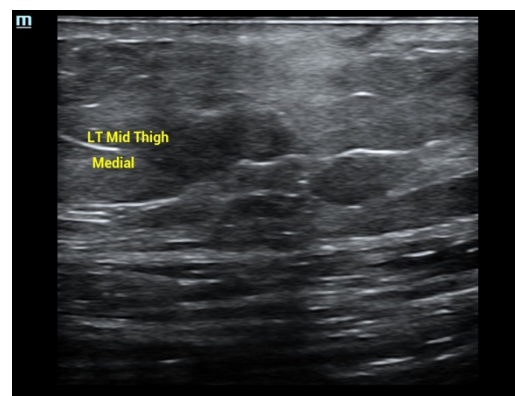


Image 82: Neovascularisation post ELVA

Spectral and colour Doppler image shows neovascularisation within a previously ablated GSV with arterialised venous flow in retrograde direction flushing the treated segment.

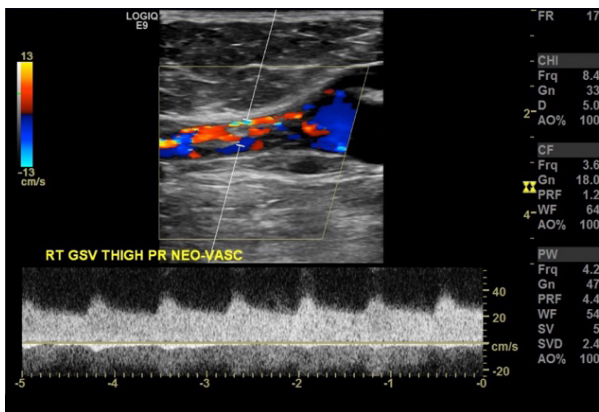


Image 83: Iatrogenic AVF

The left SFJ exhibits arteriased venous flow of high velocity and high volume due to arteriovenous fistula caused by needle injury during the administration of tumescence anaesthesia.

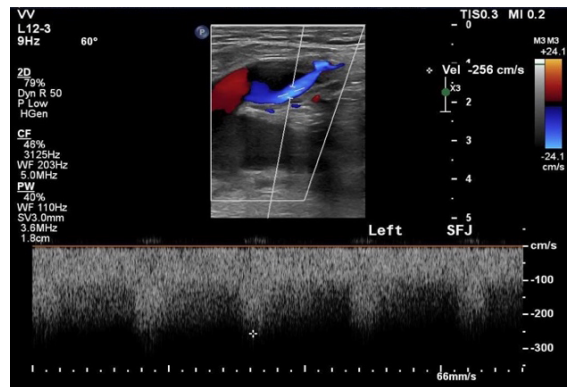


Image 84: Clinical image of the Type IV hypersensitivity in a patient who had endovenous cyanoacrylate glue ablation of the GSV

Image 85: Granuloma

B-mode image of a granuloma at the venous access site following cyanoacrylate glue ablation shows an irregularly shaped lesion with heterogeneous echogenicity and acoustic shadowing cast by the glue.

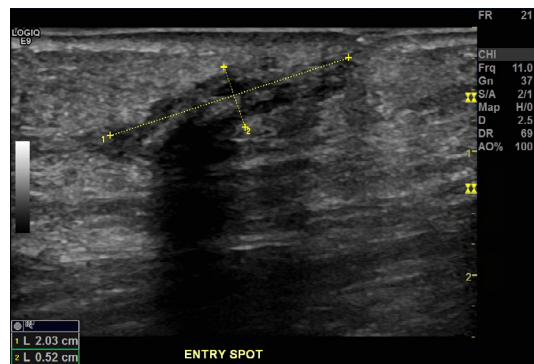


Image 86: Cellulitis

Ultrasound of the left calf with cellulitis shows hyperechoic fat lobules separated by hypoechoic fluid filled areas, commonly referred to as a "cobblestone" appearance.

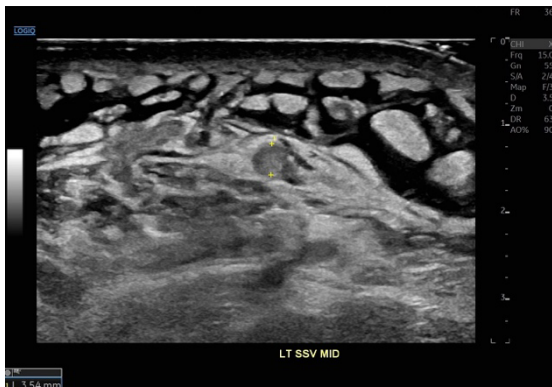


Image 87: Clinical image of a patient with leg lymphoedema

Image 88a: Venous oedema

Ultrasound image of the left posterior calf showing hypochoic area within the subcutaneous tissue, in keeping with fluid accumulation as a result of venous hypertension secondary to CVI.



Image 88b: Venous oedema

Ultrasound image of the distal calf segment of the right GSV showing hypochoic area within the subcutaneous tissue, in keeping with fluid accumulation at the gaiter area.

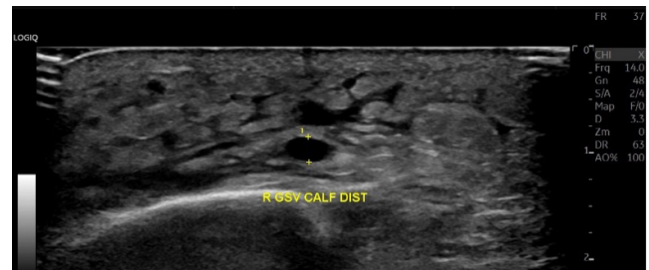


Image 89: Lymphoedema

Ultrasound image of a patient with lymphoedema shows thickened subcutaneous tissue with increased echogenicity, accompanied by multiple hypochoic areas representing fluid accumulation, characteristic of lymphoedema.

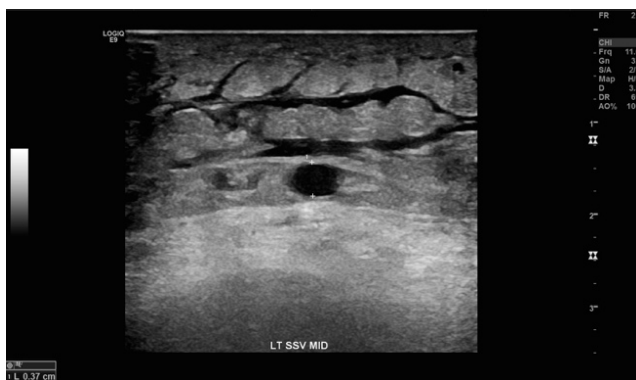


Image 90: Clinical image of a patient with leg lipoedema.

Image 91: Lipoedema

Ultrasound image of the patient's leg with lipoedema shows thickened subcutaneous fat.



Image 92: Lipoma

Ultrasound image of a lipoma shows a well-defined, hyperechoic mass within the subcutaneous tissue, with homogenous texture and smooth margins, consistent with the benign characteristics of a lipoma.



Image 93: AVM

Ultrasound image of an AVM on the right forefoot shows low resistive arterial and turbulent arterialised venous flow within the area of interest.

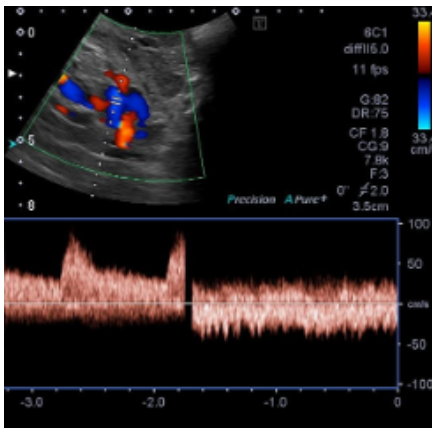


Image 94: Venous malformation

B-mode ultrasound image of an intramuscular venous malformation at the posterior thigh shows tubular, sponge like spaces within the muscle, with no evidence of thrombi.

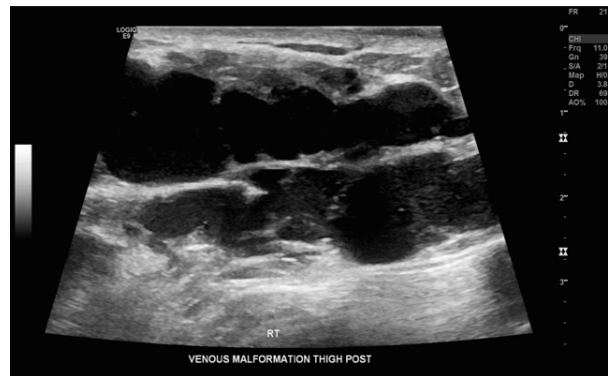


Image 95: Muscle hernia

Ultrasound image of a muscle hernia shows a focal defect in the fascia, through which a portion of the underlying muscle protrudes. The herniated muscle appears as a hypoechoic mass extending through the fascial defect, especially prominent during muscle contraction.

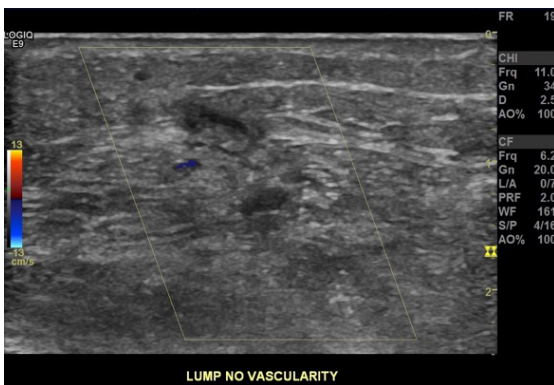


Image 96: Baker's cyst

Ultrasound image of a baker's cyst with internal echogenic material suggestive of an old haemorrhage.

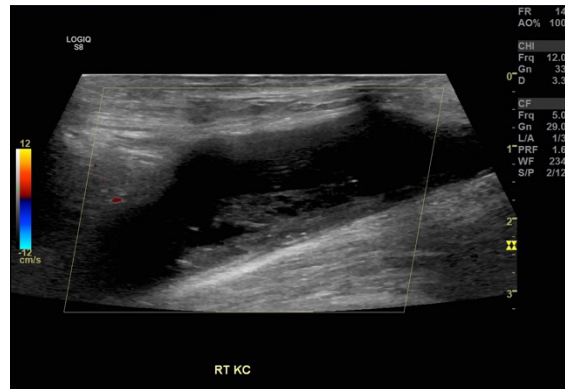


Image 97: Neuroma

Ultrasound image of the tibial nerve neuroma shows a bulbous, hypoechoic, well circumscribed mass in the tibial nerve.



Image 98: Clinical image of a patient with Klippel Trenaunay syndrome (posterior and lateral views).





Image 99: Clinical image of a patient with Klippel Trenaunay syndrome (anterior view).

Image 100: Transmitted pulsatility in the CFV

Spectral Doppler imaging of the right CFV shows spontaneous flow with pulsatile retrograde flow, suggesting a possible right sided heart problem such as tricuspid regurgitation.

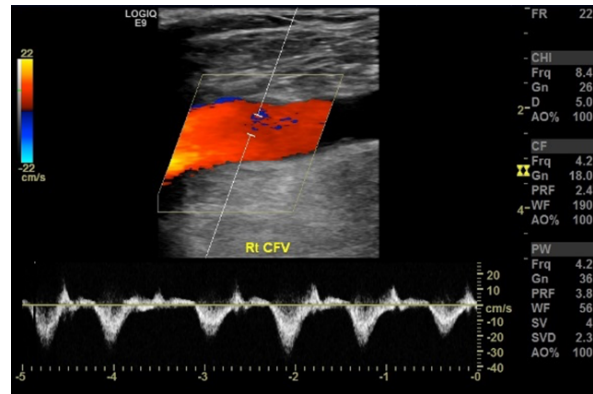
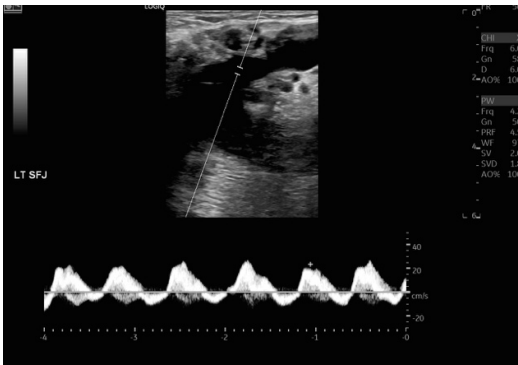


Image 101: Transmitted pulsatility at the SFJ

Spectral Doppler imaging of the left SFJ reveals pulsatile reversed flow that mimics venous reflux, indicating a possible right sided heart problem such as tricuspid regurgitation.



Room Setups



Image 102:
Room setup
with a tiltable
couch



Image 103: Room setup with a tiltable couch and an external monitor

Image 104: Room setup with a height adjustable couch, two step stool, low chair and an external monitor

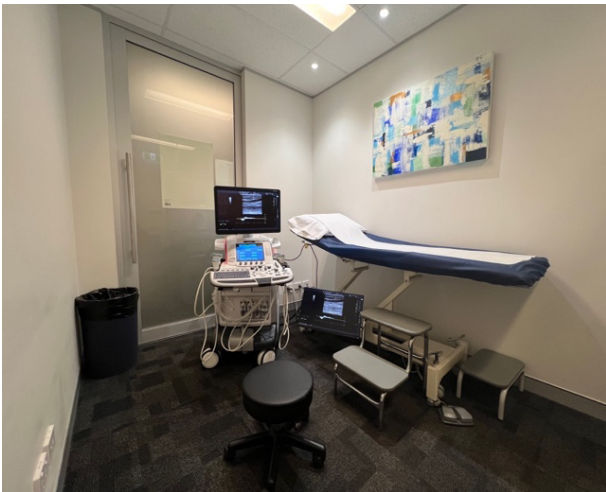


Image 105: Room setup with a height adjustable couch, two step stool, yoga ball and an external monitor

